

# Global vertical distribution of water vapor on Mars: Results from 2 Mars years of ExoMars-TGO/NOMAD science operations

**S. Aoki**, *Graduate School of Frontier Sciences, The University of Tokyo, Kashiwa, Japan* ([shohei.aoki@edu.k.u-tokyo.ac.jp](mailto:shohei.aoki@edu.k.u-tokyo.ac.jp)), **A. C. Vandaele**, **F. Daerden**, **I. R. Thomas**, **L. Trompet**, **J. T. Erwin**, **L. Neary**, **S. Robert**, **A. Piccialli**, **B. Ristic**, *Royal Belgian Institute for Space Aeronomy, Brussels, Belgium*, **G. L. Villanueva**, **G. Liuzzi**, **M. D. Smith**, *NASA Goddard Space Flight Center, 8800 Greenbelt Rd., Greenbelt, 20771 MD, USA*, **M. A. Lopez-Valverde**, **A. Brines**, **J. J. Lopez-Moreno**, *Instituto de Astrofísica de Andalucía, Glorieta de la Astronomía, Granada, Spain*, **R. T. Clancy**, *Space Science Institute, Boulder, USA*, **N. Yoshida**, *Tohoku University, Sendai, Japan*, **J. A. Holmes**, **M. R. Patel**, *School of Physical Science, The Open University, Milton Keynes, UK*, **J. Whiteway**, *Centre for Research in Earth and Space Science, York University, Toronto, Canada*, **G. Bellucci**, *Istituto di Astrofisica e Planetologia Spaziali, IAPS-INAF, Rome, Italy*.

## Introduction:

Two instruments onboard ExoMars Trace Gas Orbiter (TGO), Nadir and Occultation for Mars Discovery (NOMAD) and Atmospheric Chemistry Suite (ACS) are unique platforms to provide the global vertical distribution of trace gases (such as water vapor, carbon monoxide, hydrogen chloride, etc) on Mars from their daily solar occultation measurements (Vandaele et al., 2018; Korablev et al., 2018). The science operation of TGO has started since April 2018 and we have collected measurements for more than 2 Mars years. Here, we present the results on the vertical profiles of water vapor from the measurements by the NOMAD instrument. A full paper describing these results, Aoki et al. (2022), is currently under review.

## Dataset and analysis:

NOMAD instrument is a spectrometer working in the spectral range between 0.2 and 4.3  $\mu\text{m}$  with 3 spectral channels (2 out of 3 are in the infrared range, and the other one is in the UV-Visible range). For the analysis of water vapor presented in this study, the data taken by solar occultation measurements in the infrared channel is used. The infrared channel is composed by echelle grating and Acousto Optical Tunable Filter (AOTF), which enables us to achieve relatively high spectral resolution ( $\lambda/d\lambda \sim 17,000$ ). AOTF can instantaneously switch the observing diffraction orders, which allows us to acquire a spectrum less than every 1 second. It corresponds to the vertical sampling of less than 1 km altitudes from surface to 250 km altitude. Typically, we observe 5 or 6 different diffraction orders (i.e., spectral windows) in a single occultation. Water vapor lines are available in diffraction order 134, 136 (3011-3035  $\text{cm}^{-1}$ , 3056-3080  $\text{cm}^{-1}$ ) and order 167, 168, 169 (3752-3782  $\text{cm}^{-1}$ , 3775-3805  $\text{cm}^{-1}$ , 3797-3828  $\text{cm}^{-1}$ ). The water lines in the orders 134-136 are weaker and not heavily saturated even in the deep atmosphere so that the vertical profiles of water vapor can be retrieved from surface up to only  $\sim 90$  km altitude. The water lines in the latter spectral windows (orders 167-169) are stronger, so that the water vapor density

can be retrieved from surface up to higher altitude,  $\sim 120$  km. We have analyzed the NOMAD solar occultation data taken between April 2018 and September 2022, which corresponds to  $\text{Ls} \sim 160^\circ$  in MY 34 and  $\text{Ls} \sim 106^\circ$  in MY 36. We are continuing to process the data to cover 2 Mars years. **Fig. 1** shows the coverage of the dataset of the lower diffraction orders (the top panel) and the higher diffraction orders (the bottom panel). The total number of occultations are 5472 and 6471 for the lower and higher orders, respectively. The coverage of both spectral windows is similar since these diffraction orders are regularly observed.

The retrievals are performed with Asimut radiative transfer code (Vandaele et al., 2006). We treat each spectrum individually by assuming a constant volume mixing ratio of water vapor along the line of sight (i.e., retrievals of water vapor column density along the line of sight for each spectrum). The calibration of the solar occultation channel of NOMAD infrared has been significantly improved recently (Villanueva et al., 2022), which allows us to perform robust retrievals. We have also compared different methodologies and retrievals algorithms for the water retrievals (COPRA code developed at IAA, and PSG code developed at NASA-GSFC) and the comparison shows a good agreement (Brines et al., 2022).

## Results and discussion:

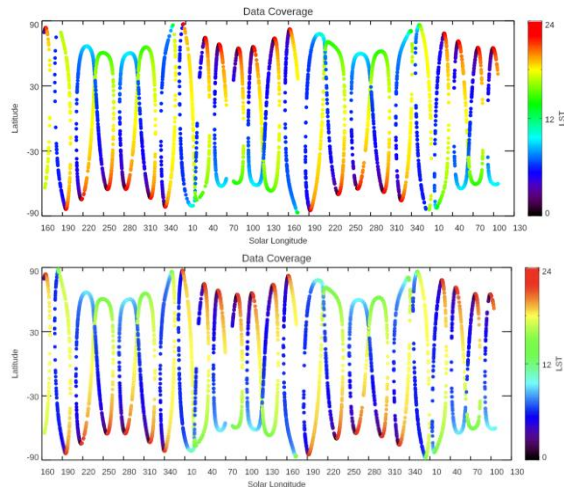
**Figure 2** and **3** show the retrieved seasonal variation of the water vapor vertical profiles from the lower orders (Fig. 2) and the higher orders (Fig. 3). For each figure, the small top panels show the latitude of the measurements (same as Fig. 1), and the middle and bottom panels exhibit the water vapor vertical profiles in the northern and southern hemispheres, respectively. As shown in Fig. 2 and 3, the results from the lower and higher orders show a very good agreement.

Fig. 2 and Fig. 3 illustrate a strong contrast between aphelion and perihelion water vertical distributions. In the aphelion periods, the water vapor is confined into very low altitudes (below 10-40 km). In

contrast, in the perihelion periods, water vapor reaches very high altitude (above 100 km). It can be explained by the fact that transport of water vapor by the global circulation is limited by the formation of ice clouds in the aphelion periods, whereas water is more effectively transported to the higher altitude and winter hemisphere in the perihelion periods because its vertical extent is less constrained by cloud formation in the warm southern summer atmosphere.

In addition to the ones in the perihelion periods, the increase of water vapor in the middle/upper atmosphere appeared around  $L_s=190^\circ$  in MY 34 and  $L_s=320^\circ-330^\circ$  in MY 34 and MY 35 are also remarkable. These periods correspond to the occurrences of the global dust storm ( $L_s=190^\circ$  in MY 34) and annual strong regional dust storms ( $L_s=320^\circ-330^\circ$ ). As shown in the earlier studies (e.g., Aoki et al., 2019; Neary et al., 2020), water vapor can reach higher altitudes when a strong dust storm occurs because the atmosphere heats up due to the presence of dust and it prevents water from condensing as ice clouds. These results also confirm that dust storms and the southern summer are the main events for water vapor to reach middle/high altitude as shown by earlier studies (Fedorova et al., 2020; Villanueva et al., 2021).

**Figures:**



**Figure-1:** Coverage of the solar occultation measurements by NOMAD used in this study. The top panel is the data taken in orders 134 and 136, and the bottom panel is orders 167-169. X-axis is solar longitude (from MY 34 to MY 36), and Y-axis is latitudes. The difference in color indicates the local time.

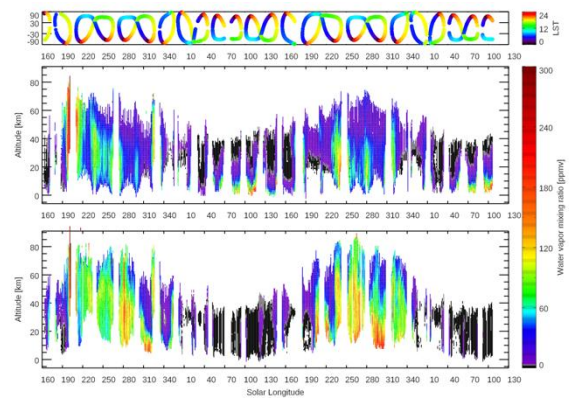


**Figure-2:** Vertical profiles of water vapor in the unit of volume mixing ratio retrieved from orders 134 and 136 of NOMAD measurements. The top, middle, and bottom panels show the latitude and local solar time of the measurements, water vapor vertical profiles in the northern hemisphere, and southern hemisphere, respectively.

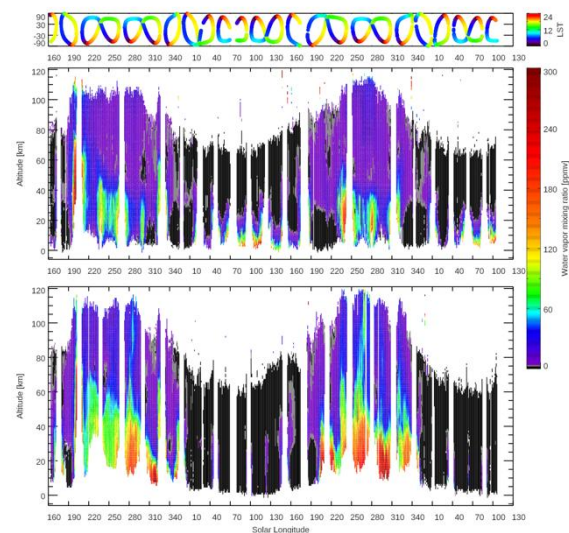


**Figure-3:** Same as Fig. 2 but retrieved from orders 167-169 of the NOMAD measurements.

### Bibliography:

Aoki, S., et al. (2019), Water vapor vertical profiles on Mars in dust storms observed by TGO/NOMAD. *J. Geophys. Res.: Planets*, 124, 3482-3497, doi:10.1029/2019JE006109.

Aoki, S., et al. (2022), Global vertical distribution of water vapor on Mars: Results from 3.5 years of ExoMars-TGO/NOMAD science operations. *J. Geophys. Res.: Planets*, *under review*.

Brines, S., et al. (2022), Water vapor vertical distribution on Mars during perihelion season of MY34 and MY35 with ExoMars-TGO/NOMAD observations. *J. Geophys. Res.: Planets*, *under review*.

Fedorova, A. A., et al. (2020), Stormy water on

Mars: The distribution and saturation of atmospheric water during the dusty season. *Science*, Vol. 367, Issue 6475, pp. 297-300, doi: 10.1126/science.aay9522.

Korablev, O., et al. (2018), The Atmospheric Chemistry Suite (ACS) of Three Spectrometers for the ExoMars 2016 Trace Gas Orbiter, *Space Science Reviews*, 214, 1, article id. 7, 62, doi: 10.1007/s11214-017-0437-6.

Neary L., et al., (2020), Explanation for the increase in high altitude water on Mars observed by NOMAD during the 2018 global dust storm, *Geophys. Res. Lett.*, 47, e2019GL084354, doi:10.1029/2019GL084354.

Vandaele, A. C., et al., (2006), Simulation and retrieval of atmospheric spectra using ASIMUT, paper presented at Atmospheric Science Conference, Eur. Space Agency, Frascati, Italy.

Vandaele, A. C., et al., (2018), NOMAD, an integrated suite of three spectrometers for the ExoMars Trace Gas mission: technical description, science objectives and expected performance, *Space Science Reviews*, 214, 5, article id. 80, 47 pp, doi: 10.1007/s11214-018-0517-2.

Villanueva, G., L. et al., (2021). Water heavily fractionated with altitude on Mars as revealed by ExoMars/NOMAD, *Science Advances*, Vol. 7, no. 7, eabc8843, DOI: 10.1126/sciadv.abc8843

Villanueva, G., L. et al., (2022). The deuterium isotopic ratio of water released from the Martian caps as measured with TGO/NOMAD, *Geophysical Research Letters*, *under review*